

# Line Art Correlation Matching Network for Automatic Animation Colorization

Zhang Qian  
Wang Bo  
Wen Wei  
Li Hai  
Liu Junhui



Figure 1: Animation sequence colorization example. The first row shows a sketch sequence, the second row shows the colored frames generated by our network conditioned on the colored frame in the first column, the third row shows the original animation frames. The example sequence is from the film *Princess Mononoke*.

## ABSTRACT

Automatic animation line art colorization is a challenging computer vision problem, since the information of the line art is highly sparse and abstracted and there exists a strict requirement for the color and style consistency between frames. Recently, a lot of Generative Adversarial Network (GAN) based image-to-image translation methods for single line art colorization have emerged. They can generate perceptually appealing results conditioned on line art images. However, these methods can not be adopted for the purpose of animation colorization because there is a lack of consideration of the in-between frame consistency. Existing methods simply input the previous colored frame as a reference to color the next line art, which will mislead the colorization due to the spatial misalignment of the previous colored frame and the next line art especially at positions where apparent changes happen. To address these challenges, we design a kind of correlation matching model (called

CM) to align the colored reference in a learnable way and integrate the model into an U-Net structure generator in a coarse-to-fine manner. This enables the generator to reconstruct the layer-wise synchronized features from the deep semantic code to the content progressively. Extension evaluations show that CM model can effectively improve the in-between consistency and the quality of colored frames especially when the motion is intense and diverse.

## CCS CONCEPTS

•Computing methodologies → *Matching*; **Matching**;

## KEYWORDS

Animation Colorization, Sketch Correlation, Image Translation

### ACM Reference format:

Zhang Qian, Wang Bo, Wen Wei, Li Hai, and Liu Junhui. 2020. Line Art Correlation Matching Network for Automatic Animation Colorization. In *Proceedings of MM'20: ACM Multimedia 2020, NI, NI, June 03–05, 2020 (MM '20)*, 9 pages.  
DOI: 10.1145/1122445.1122456

Permission to make digital or hard copies of all or part of this work for personal or classroom use is granted without fee provided that copies are not made or distributed for profit or commercial advantage and that copies bear this notice and the full citation on the first page. Copyrights for components of this work owned by others than ACM must be honored. Abstracting with credit is permitted. To copy otherwise, or republish, to post on servers or to redistribute to lists, requires prior specific permission and/or a fee. Request permissions from [permissions@acm.org](mailto:permissions@acm.org).

MM '20, NI, NI

© 2020 ACM. 978-1-4503-XXXX-X/18/06...\$15.00  
DOI: 10.1145/1122445.1122456

## 1 INTRODUCTION

Nowadays, animation has become part of our daily entertainments, thousands of animations have accounted for a large proportion of the global viewership both on TV and online video platforms.

According to the AJA's 2018 report [1], the popularity of animation is still growing. Six years of continuous growth has been seen in Japan's anime market. However, animation production is a complex and time-consuming process that requires a large number of workers to collaborate in different stages. The key-frame sketches that define the major character movements are portrayed by lead artists while the in-between sketches of motions are completed by inexperienced artists. Then, the labor workers repetitively colorize all the line arts on the basis of the character's color chart previously designed by the lead artists. This colorization procedure is considered to be a tedious and labor-intensive work. Thus, finding an automatic method to consistently colorize the sketch frames can significantly improve the efficiency of animation production and greatly save the expenses and labour cost.

The image-to-image translation method presented by Isola et al [11] utilize Generative Adversarial Networks (GANs) to learn a mapping model from the source image domain to the target image domain. The similar idea has been applied to various tasks such as generating photographs from attribute and semantic distributions. There has been a lot of learning based methods [3, 5–7, 9, 11, 13, 16, 17, 33, 34, 36] for single sketch colorization, most of which treat the problem as an image-to-image translation task, aiming at generating a perceptual pleasing result. However, due to the lack of consideration of the in-between consistency, this kind of methods can not be directly adopted to colorize frame sequences.

In [27], temporal informations are incorporated into the image-to-image translation network to encourage the consistency between colorized frames by simply taking the previous colored frame as an input to predict the current colored frame. Two problems exist in these methods. Firstly, the semantic distribution between the previous colored frame and the current sketch frame is misaligned in the spatial domain, which will mislead the colorization, especially at positions where apparent changes happen. Secondly, although information of the previous colored frame and the current sketch frame is used to do prediction, information of the previous sketch which is highly related to both the previous colored frame and the current sketch is ignored.

To address the above problems, we propose a coherent line art colorization framework with a learnable correlation matching model (called CM) to match the correlation in feature maps. The CM model utilizes two kinds of consistencies of four frames, which consist of the domain style consistency and the spatial content consistency. On the one hand, because of the domain style consistency between the previous and next line art, the in-between content transformation can be presented by the correlation of continuous frames. On the other hand, because of the spatial content consistency of the next line art and colored image, we assume that the in-between motion can be maintained across two style domains obviously. Therefore, the transformation can be applied to color domain to reconstruct the target image from semantic or texture patches of the previous color image. To simulate the animation colorization behaviour that artists usually determine the global color composition before local details, we integrate a series of CM models into a coarse-to-fine decoder. Simultaneously, we introduce a network to decrease the matching difficulty brought by the serious sparsity of line art. Overall, our contributions are as follows:

- We propose a learnable CM model to reconstruct the target color image by matching the correlation of feature maps and applying the in-between motion to the color domain.
- We design a coherent line art sequence colorization framework consisting of four encoders and one decoder, which can generate high-quality colorized images effectively and efficiently.
- We devise a method to build diverse and discriminative datasets from cartoon films for the coherent frame sequence colorization task.

## 2 RELATED WORK

### 2.1 Sketch Line Art Colorization

Recently, GAN[19] has offered superior quality in generation tasks compared to conventional image generation methods. Several studies have been conducted on GAN for line art colorization, which train CNNs on large datasets to combine low-level local details and high-level semantic information to produce a perpetual appealing image. Isola et al[11], Zhu et al [36] and Chen et al [3] learn a direct mapping from human drawn sketches (for a particular category or with category labels) to realistic images with generative adversarial networks. PaintChainer [17] develops an online application that can generate pleasing colorization results for anime line arts based on an U-Net structure generator. A [5] improves colorization quality by adding an independent local feature network to the generator. To increase the color diversity and control the style of image, reference are added to the generator. In [5, 34], points or lines with specified colors are input to a generator as hints to change color layouts of the target drawing positions or areas. In [7], a color palette is used to guide the color distribution of the result. In [33], the VGG features of the sample image is added to the generator as a style hint. Style2Paints [34] extends the method by adding a refinement stage, which provides a state-of-the-art result in single sketch colorization.

However, none of these works can be directly transplanted to the frame sequence colorization. Since no meticulous-designed dense reference has been introduced to affect details of the result, rigid color consistency required in the frame sequence colorization task can not be well guaranteed. Thasarathan et al [27] is the first study working on colorizing sketch frame sequences, which takes the previous colored image as a dense reference and simply concatenates it with the sketch as an input of the encoder. This will mislead the colorization because of the spatial misalignment between a sketch and the corresponding color reference. In this paper, we reconstruct the aligned color reference by finding the correlation of sketch features.

### 2.2 Traditional Sketch Correlation

Despite a strong correlation between every two adjacent frames, finding the correction between sketches is a difficult task, because features of sketches are sparse and highly-abstracted. Some studies [22, 24, 30, 35] assume that the line art is closed and can be segmented into different shape areas, and they use shapes and topological features to find the correlation between adjacent sketches. Some other studies [18, 25, 26] are proposed to model the correspondence between two frames as a as-rigid-as-possible deformation,

which is iteratively found by matching local features. Those methods can not handle complex sketch changes, because they depend on the stability of shapes, topology or local features, which often varies from adjacent animation frames.

### 2.3 Deep CNN Feature Matching

Another way to find the correspondence between images is deep feature matching. Local patches in deep features have characteristic arrangements of feature activations to describe objects, and higher-up code becomes more invariant under in-class variation [14]. It has been shown in high-level image recognition tasks that such deep features are better representations for images [32]. Li et al [14] realizes the image-to-image translation between photograph and style image via matching local patches of features extracted from a pre-trained VGG network. In order to transfer an image  $I$  of domain  $A$  to domain  $B$ , the features of domain  $B$  is aligned to the content of image  $I$  by matching the patches of deep features, and then the transferred image is reconstructed from aligned features. Liao et al [15] formulates the transfer mapping as a problem of image analogies [4, 10] by separating the matching into one in-place mapping (spatial invariant) and one similar-appearance mapping (style invariant) to improve the transfer quality and precision. The pre-trained VGG network can offer adequate semantics for correct patch matching, but it only adapts general photographs instead of sparse and highly-abstracted sketch representations. In order to learn effective sketch features, we design a learnable correlation matching model and integrate it to our generator for training. This module will guide the network to learn a good representations for the sketch frame sequence colorization task by itself.

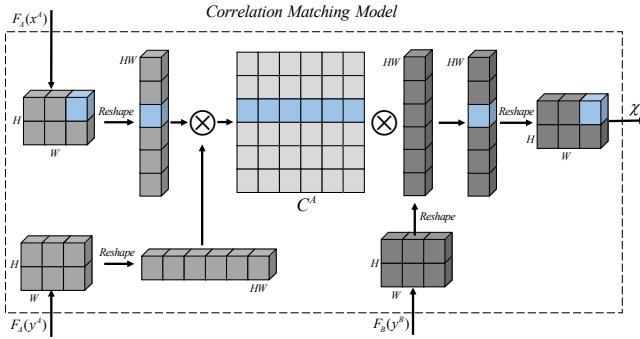


Figure 2: An illustration of correlation matching (CM) model

## 3 METHOD

This section describes the proposed line art sequence colorization method shown in Figure 4. We first build the learnable matching model called correlation matching model, which can account for consistency between frames to take into consideration temporal information. Then, we propose the line art correlation matching network(LCMN) to integrate a series of CM models that can act on semantic or texture features.

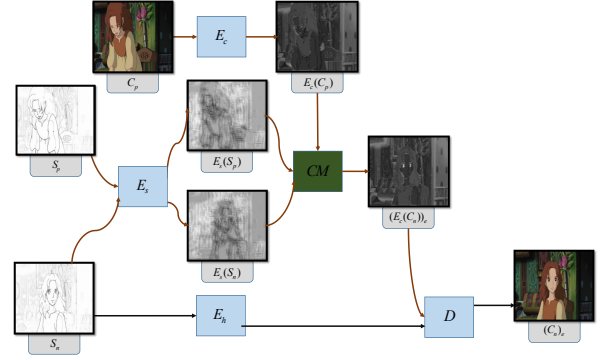


Figure 3: Overview of our network. There are mainly 4 encoders and 1 decoder in our network. Encoder  $E_h$  and decoder  $D$  compose an U-Net structure, which is our backbone network. The previous colored image  $c_p$  is encoded by  $E_c$  as  $E_c(C_p)$ , the previous sketch and the current sketch are encoded by  $E_s$  as  $E_s(S_p)$  and  $E_s(S_n)$  respectively. Then, in CM model,  $E_s(S_p)$  and  $E_s(S_n)$  are matched to generate a mapping matrix which is used to warp  $E_c(C_p)$  to  $(E_c(C_n))_e$ . Taking  $(E_c(C_n))_e$  as a dense estimation of  $E_c(C_n)$ , we reconstruct the estimation of  $C_n$  by integrating  $(E_c(C_n))_e$  to the decoder  $D$ .

### 3.1 Correlation Matching Model

Similar to the representation in [15], let  $x^A, y^A \in \mathbb{R}^{H' \times W' \times 3}$  be two images in style domain  $A$ , let  $x^B, y^B \in \mathbb{R}^{H' \times W' \times 3}$  be two images in style domain  $B$ . We arrange  $x^A, y^A, x^B, y^B$  as image analogy  $x^A : x^B :: y^A : y^B$ , where  $x^B$  are unknown variable. This analogy implies two constraints: 1)  $x^A$  and  $x^B$  (also  $y^A$  and  $y^B$ ) correspond at the same spatial content; 2)  $x^A$  and  $y^A$  (also  $x^B$  and  $y^B$ ) are similar in style (color, lighting, texture and etc). Let  $F_A(x^A), F_A(y^A), F_B(x^B), F_B(y^B)$  be the corresponding DCNN features of  $x^A, y^A, x^B, y^B$ , where  $F_A(\cdot), F_B(\cdot) \in \mathbb{R}^{H \times W \times L}$ , our goal is to build a learnable network structure to find the correlation matrix  $C^A \in \mathbb{R}^{HW \times HW}$  of  $F_A(x^A)$  and  $F_A(y^A)$ , then using  $F_B(y^B)$  and the matrix  $C^A$  to reconstruct the unknown  $F_B(x^B)$ .

Firstly, let  $i \in HW$  and  $j \in HW$  denote the index of spatial positions of the image features. Each element  $C_{i,j}^A$  represents the correlation intensity between position  $i$  in  $F_A(x^A)$  and position  $j$  in  $F_A(y^A)$ , and it is calculated as below:

$$C_{ij}^A = f(F_A(x^A)_i, F_A(y^A)_j), \quad (1)$$

in which  $f$  denotes a kernel function computes the similarity of the scalars. We apply the gaussian function in this paper ( $f(a, b) = e^{-a^T b}$ ). As  $x^A$  and  $y^A$  are in the same style domain, the local pixels with the similar semantic content are similar in features, the correlation can be represented as similarities. Then, we estimate the feature  $F_B(x^B)$  by matching the pixels from  $F_B(y^B)$  and the estimation of  $F_B(x^B)$  is written as  $\chi$ . Each pixel in  $\chi$  is resumed by

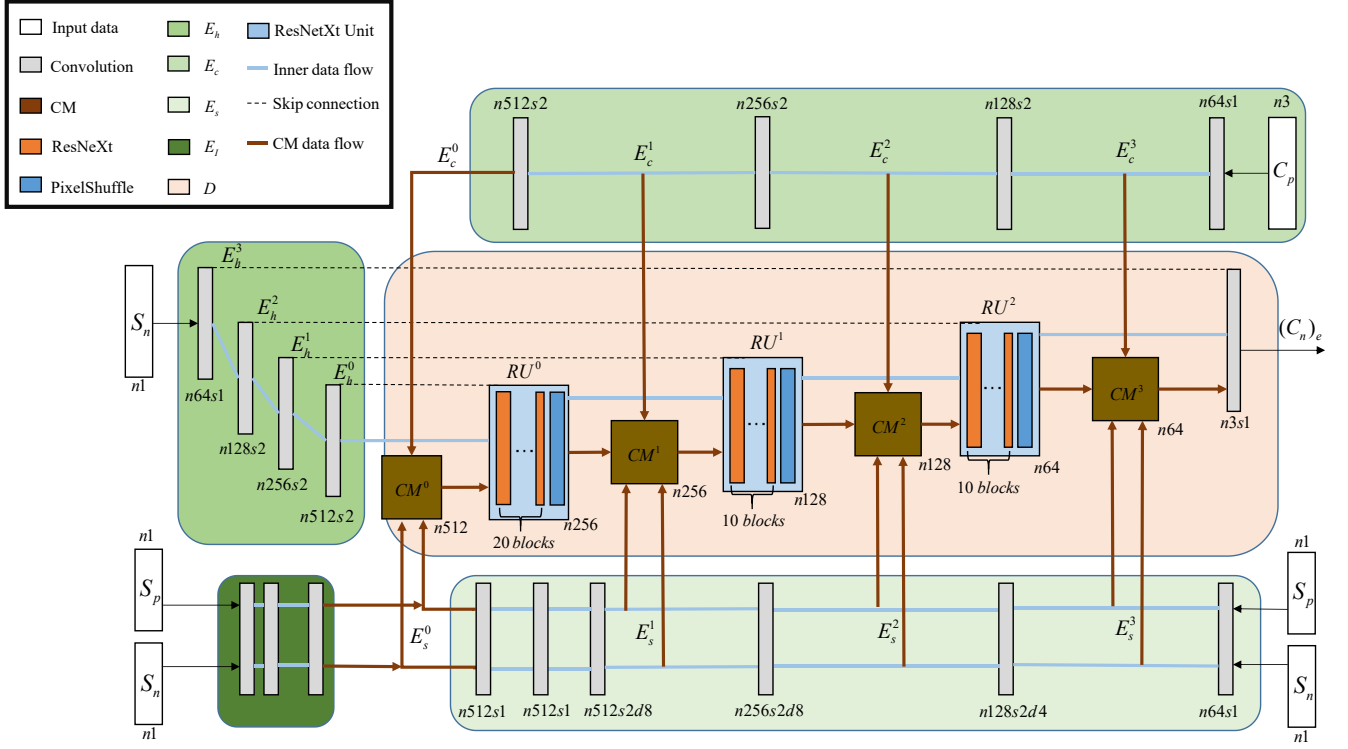


**Figure 4: Architecture of our generator Network with corresponding number of feature maps ( $n$ ), stride ( $s$ ) and dilation ( $d$ ) indicated for each convolutional block**

accumulating all the pixels in  $F_B(y^B)$  as follows:

$$\chi_i = \sum_{\forall j} w_{ij} F_B(y^B)_j, \quad (2)$$

$$w_{ij} = \frac{1}{\sum_{\forall j} c_{ij}^A} c_{ij}^A, \quad (3)$$

in which  $w_{ij}$  denotes the weight of the pixel  $j$  in  $F_B(y^B)$  to reconstruct the unknown feature pixel  $F_B(x^B)_i$ . Notice that  $C_{ij}^B$  is necessary to precisely reconstruct the  $F_B(x^B)$ . However, we replace it with  $C_{ij}^A$  feasibly, since  $x_A$  and  $x_B$  (also  $y_A$  and  $y_B$ ) contain the same spatial content. Equation 1 and 2 can be summarized as follow:

$$\begin{aligned} \chi_i &= CM(F_A(x^A), F_A(y^A), F_B(y^B))_i \\ &= \frac{1}{\sum_{\forall j} f(F_A(x^A)_i, F_A(y^A)_j)} \sum_{\forall j} f(F_A(x^A)_i, F_A(y^A)_j) F_B(y^B)_j. \end{aligned} \quad (4)$$

Equation 4 is called correlation matching (CM) model, which reconstruct the unknown  $F_B(x^B)$  with  $F_A(x^A)$ ,  $F_A(y^A)$  and  $F_B(y^B)$ . CM model can be integrate to the generator of the image-to-image domain translation task. Different from the matching procedure in [15] and [14], the matching model will guide the learning of DCNN features. Allowing the network to be able to learn a matching-friendly and task-friendly deep feature from the whole dataset instead of a few images will improve the robustness and accuracy

for a given task. Figure 2 shows the calculation process of the CM model. In the next section, we will introduce the temporal reference in a coarse-to-fine manner by applying CM model to the frame colorization task.

### 3.2 Line Art Correlation Matching Network

As for the coherent sketch frame colorization, the analogy can be written as  $S_p : C_p :: S_n : C_n$ , in which  $S_p$  ( $S_n$ ) and  $C_p$  ( $C_n$ ) represent the previous (current) sketch frame and previous (current) color frame respectively. Our generator takes  $S_n$  as input conditioned on previous frame pair  $S_p$  and  $C_p$  and returns a color estimation  $C_e$  temporally consistent to the previous colored frame. This step can be summarized as the following formula:

$$C_e = G(S_p, C_p, S_n). \quad (5)$$

U-Net[20] structure has recently been used on a variety of image-to-image translation tasks [11][36][5]. In an U-Net network structure, the features of the encoder are directly added to the decoder by skip connections.

In our task, however, the encoding feature of the  $C_p$  can not be directly added to the decoder for decoding  $C_n$ , because of the spatial inconsistency. We aim to align the feature of  $C_p$  to  $C_n$  and add the aligned feature to the decoder in a coarse-to-fine manner with the help of the CM model.

As shown in Figure 4, our generator consist of four encoders and one decoder. The backbone of our network( $E_h$  and  $D$ ) is an

U-Net structure. The input of the encoder  $E_h$  is the current sketch frame  $S_n$ , which contains four convolution layers that progressively halved the feature spatially from  $256 \times 256$  to  $32 \times 32$ . As for the decoder  $D$ , inspired by [5], we stack the ResNeXt blocks [29] instead of Resnet blocks [8] to effectively increase the capacity of the network and use the sub-pixel convolution layers [23] to increase the resolution of the features after each ResNeXt blocks. We represent each combination of ResNeXt blocks and sub-pixel convolution layer as  $RU$  in our paper. Two extra encoders are introduced to encode sketches and colored images respectively, called  $E_s$  and  $E_c$ .  $E_c$  has the the same structure as  $E_h$  and  $E_s$  consists of 6 convolution layers. We add dilation [31] to each layers of  $E_s$  to increase the receptive fields, which will enable the network to further learn some nonlocal topology features of the sketch. Inspired by [5], we introduce a extra pre-trained sketch classification network  $E_I$  to bring more abundant semantic implications to the matching process. We use the activations of the 6-th convolution layer of the Illustration2Vec network [21] that is pretrained on 128w illustrations including colored images and line art images. The decoder  $D$  mixes the encoding features and reconstructs the color result from a coarse-to-fine manner. In each resolution layer of the decoder, there exists a CM model to accumulate the encoded features.

As shown in Figure 4, the intermediate output of  $E_s$  ( $E_c$ ) is denoted as  $E_s^3, E_s^2, E_s^1, E_s^0$  ( $E_c^3, E_c^2, E_c^1, E_c^0$ ), the intermediate code of  $E_h$  is denoted as  $E_h^3, E_h^2, E_h^1, E_h^0$ . The CM model of each resolution is represented as  $CM^0, CM^1, CM^2, CM^3$ . In the first CM model( $CM^0$ ), we aim to estimate the unknown feature  $E_c^0(C_n)$  by aligning  $E_c^0(C_p)$  in spatial domain, and we call the prediction result  $(E_c^0(C_n))_e$ . In order to make the matching more accurate and robust, we concatenate  $E_s^0$  with  $E_I$  as the matching feature so that the caculation of model  $CM^0$  can be written as Equation 6 (we represent the concatenate operation as  $ca()$ ).

$$\begin{aligned} (E_c^0(C_n))_e &= CM^0(ca(E_s^0(S_n), E_I(S_n)), ca(E_s^0(S_p), E_I(S_p)), E_c^0(c_p)) \\ &= CM(ca(E_s^0(S_n), E_I(S_n)), ca(E_s^0(S_p), E_I(S_p)), E_c^0(c_p)) \end{aligned} \quad (6)$$

The predicted  $(E_c^0(C_n))_e$  contains the same style as  $E_c^0(C_p)$  and it is consistent with the  $E_h^0(S_n)$  in spatial domain, which makes the  $(E_c^0(C_n))_e$  a good reference for the network to further construct the higher resolution features. We concatenate the  $(E_c^0(C_n))_e$  with  $E_h^0(S_n)$  and input it to the first ResnetXT upsample block( $RU^0$ ) to further reconstruct the higher resolution features. We treat the output of  $RU^0$  as a coarse estimation of  $E_c^1(C_n)$ , so now we have the analogy as  $E_s^1(S_n):RU^0::E_s^1(S_p):E_c^1(C_p)$ . We can match  $RU^0$ ,  $E_s^1(S_n)$  with  $E_c^1(C_p)$ ,  $E_s^1(S_p)$  to reconstruct a more accurate prediction  $(E_c^1(C_n))_e$  and thus the calculation of  $CM^1$  can be represented as Equation 7:

$$\begin{aligned} (E_c^1(C_n))_e &= CM^1(RU^0, E_s^1(S_n), E_c^1(C_p), E_s^1(S_p)) \\ &= CM(ca(RU^0, E_s^1(S_n)), ca(E_c^1(C_p), E_s^1(S_p)), E_c^1(c_p)). \end{aligned} \quad (7)$$

Let  $k$  denotes the label of the layer of the CM model, for  $k > 1$ . Since we can treat each  $RU^{k-1}$  as a coarse estimation of corresponding  $E_c^k(C_n)$ , the rest CM model ( $CM^2$  and  $CM^3$ ) can be induced from Equation of  $CM^1$ . Then, we write the calculation in an united

Equation 8:

$$\begin{aligned} (E_c^k(C_n))_e &= CM^k(RU^{k-1}, E_s^k(S_n), E_c^k(C_p), E_s^k(S_p)), k > 1. \quad (8) \\ &= CM(ca(RU^{k-1}, E_s^k(S_n)), ca(E_c^k(C_p), E_s^k(S_p)), E_c^k(c_p)) \end{aligned}$$

From Equation 8, we can discover that the features of  $C_p$  is aligned to  $C_n$  in a coarse-to-fine manner. With the increasing of the feature resolution, more detailed information in features is considered for matching and a more fine result can be reconstructed. At the end of the decoder, we use two convolution layers to decode the aligned features to the RGB color domain.

### 3.3 Loss Objective

**Color Loss.** We apply a color loss to the output of the generator  $G$  and the ground truth image using the following objective function:

$$L_1(G) = \mathbb{E}_{X, Y} \|Y - G(X)\|_1, \quad (9)$$

where  $X = (C_p, S_p, S_n)$  and  $Y = C_n$

**Perceptual Loss.** While using only the  $L1$  loss will make the generated result blurry, perceptual loss can help the model to better reconstruct fine details and edges[12]. We calculate the perceptual loss on the feature maps of the VGG-19 model pre-trained on ImageNet at different depths.

$$L_{VGG}(G) = \sum_{f \in F} \|VGG_f(Y) - VGG_f(G(X))\|_2 \quad (10)$$

where  $F$  is the set of depths of VGG-19 which are considered, in our case  $F = 1, 3, 5, 9, 13$ .

**Objective.** By combing all the mentioned losses, the final objective function can be represented as follows:

$$L_G = \lambda_1 L_1 + \lambda_2 L_{VGG}, \quad (11)$$

where  $\lambda_1, \lambda_2$  influence the relative importance of the different loss functions.

### 3.4 Implementation Details

The inputs of  $CM^3$  are two size  $256 \times 256$  feature maps and the shape of the relevent correlation matrix is  $65536 \times 65536$ , which will cause the memory overhead for a single GPU and also greatly extend the training and inferring time. Thus we remove the  $CM^3$  model in our implementation by directly connecting the output of  $RU^2$  to the last convolution layers.

## 4 EXPERIMENT

### 4.1 Experimental Setup

**Dataset.** We collect 10 different cartoon films of Hayao Miyazaki (*Howl's Moving Castle*, *Whisper of the Heart*, *The Wind Rises*, *Ki-ki's Delivery Service*, *Porco Rosso*, *My Neighbor Totoro*, *The Secret World of Arrietty*, *Spirited Away*, *Princess Mononoke*, *Ponyo*), three of which (*The Secret World of Arrietty*, *Whisper of the Heart*, *My Neighbor Totoro*) are used for training and the rest for testing. We divide these training films into shots by utilizing the method described in[2]. Since frames from two different shots may not be strongly correlated and mislead the training process, we only extract training frame pairs from the same shot. In order to train the model to handle more diverse and intense frame variations, we design a strategy to extract more differential training pairs from a single



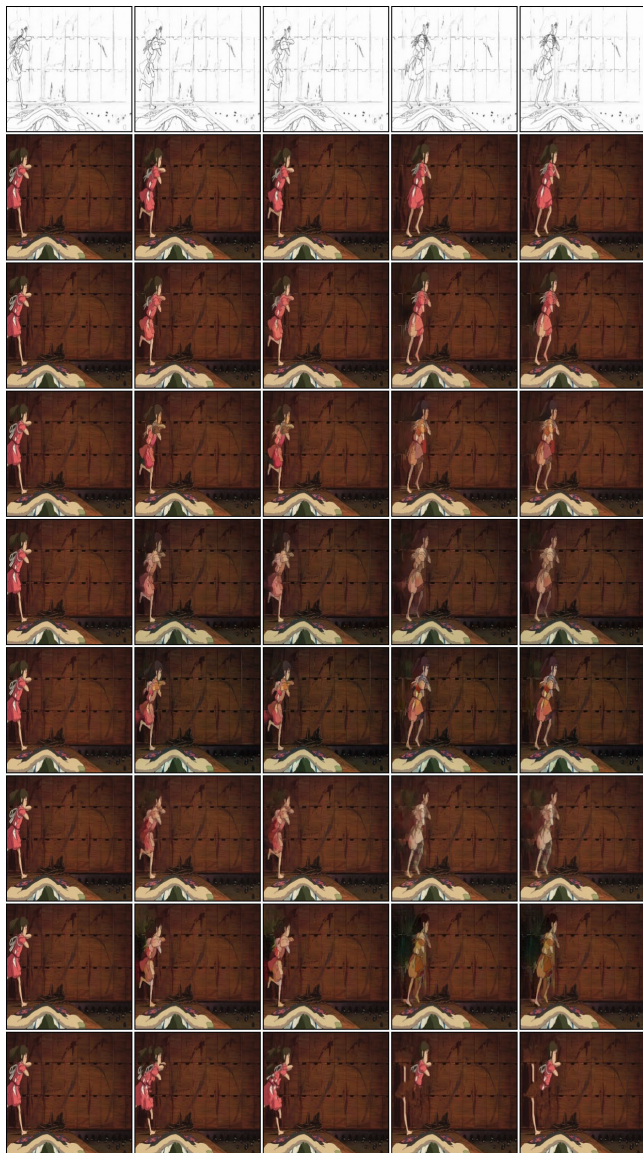


**Figure 5: Example of all the compared method at stride=1, from top to bottom is the ground truth and the results of LCMN, LCMN (w/o CM), TCVC (our loss), TCVC, Pix2Pix (with ref/our loss), Pix2Pix (with ref), DeepAnalogy. The first column of each rows is the origin colored image, and the successive colour is the predicted frame conditioned on the first colored reference. The example sequence is from the film *Spirited Away***

shot. We apply a sliding window to every sequence to obtain the frame pairs, first of which is the start frame of the window, and second of which is the last frame of the window. The stride of window is set to 5, and the width is set to 40. In this way, we extract 60k pairs of training color frames and then convert this color frame set to simulate artificial line art by paintchainer’s LeNet [17] and take it as the sketch training set.

**Table 1: PSNR/SSIM result of frame sequence with stride=1**

method	frame1( $iv:1$ )	frame2( $iv:2$ )	frame3( $iv:3$ )	frame4( $iv:4$ )
LCMN	<b>30.24/0.9790</b>	<b>29.10/0.9747</b>	<b>28.24/0.9710</b>	<b>27.89/0.9688</b>
LCMN(w/o CM)	29.44/0.9731	28.06/0.9675	27.28/0.9629	26.93/0.9602
TCVC(our loss)	23.45/0.9086	22.78/0.9026	22.50/0.8989	22.37/0.8970
TCVC	23.73/0.9164	23.05/0.9107	22.77/0.9073	22.64/0.9055
pix2pix(with ref/our loss)	29.76/0.9593	27.98/0.9530	26.74/0.9471	26.30/0.9441
pix2pix(with ref)	28.59/0.95594	26.82/0.9510	25.65/0.9433	25.20/0.9394
DeepAnalogy	29.90/0.9773	27.22/0.9701	26.14/0.9645	25.79/0.9629

**Parameter Setting.** Our proposed method is implemented in PyTorch, and trained and tested on a single Tesla P40 GPU. For every experiment, we feed our network with input resized to  $256 \times 256$  for 40 epochs, and the batch size is set to 2. We use the Adam optimizer with the momentum terms  $b1 = 0.5$  and  $b2 = 0.9$ , and the initial learning rate for Adam optimizer is  $1e - 4$ . For hyper-parameters setting, we fix  $\lambda_1 = 10$  and  $\lambda_2 = 2e - 2$ .

**Evaluation Metric.** In order to validate results of our method, we employ Structural Similarity Index (SSIM) [28] and Peak Signal to Noise Ratio (PSNR) metrics to evaluate the difference between the generated images and the ground truth frames.

## 4.2 Model Analysis

In the subsection, we investigate the influence of the CM model. We gather all the shots of 7 test films into a shots set (7000 shots total). To see how the motion intensity and diversity influence the result, for each shot, we randomly selected 5 continuous frames at a stride of  $S$ , which is varied from 1 to 10. Obviously, the intervals between the reference frame and the generated frames range from frame 1 to 40 (the interval is represented as  $iv$  in tabel). We take the first frame of this sequence as the color reference for the model to predict the successive frame. We eliminate the sequence from the test dataset when there exist an unchanged frame compared with the first frame, since it is not nessasery to predict the colorization when no change happens. We also eliminate the sequence from the test dataset when big region of uncorrected semantics shows up (for example, an character not shown in the first frame suddenly comes in in the following frames), these data will degenerate the test since the right color of the unknown semantic object is generally uncertain. After the elimination, we get a dataset of 3500 shot sequences for testing. Tabel 1,2,3 have show the result of the evaluation and Figure 5, 6, 7 have show the examples of the results.

To evaluate the influence of correlation mathing model, we completely remove CM models from the LCMN network, and directly concatenate the output of each  $RU$  model to the successive  $RU$ . As shown in Table 1, there is a relatively smaller advantage of LCMN over LCMN (w/o CM) when the interval is less than 5. This is because most of the test sketch cases only change slightly and locally between coherent frames when the interval is small, and some unknown part of frames can be easily predicted by the local ability of the network. However, when we increase the interval to enhance the motion intensity and diversity, LCMN is apparently better than LCMN (w/o CM) as shown in Table 2, 3.

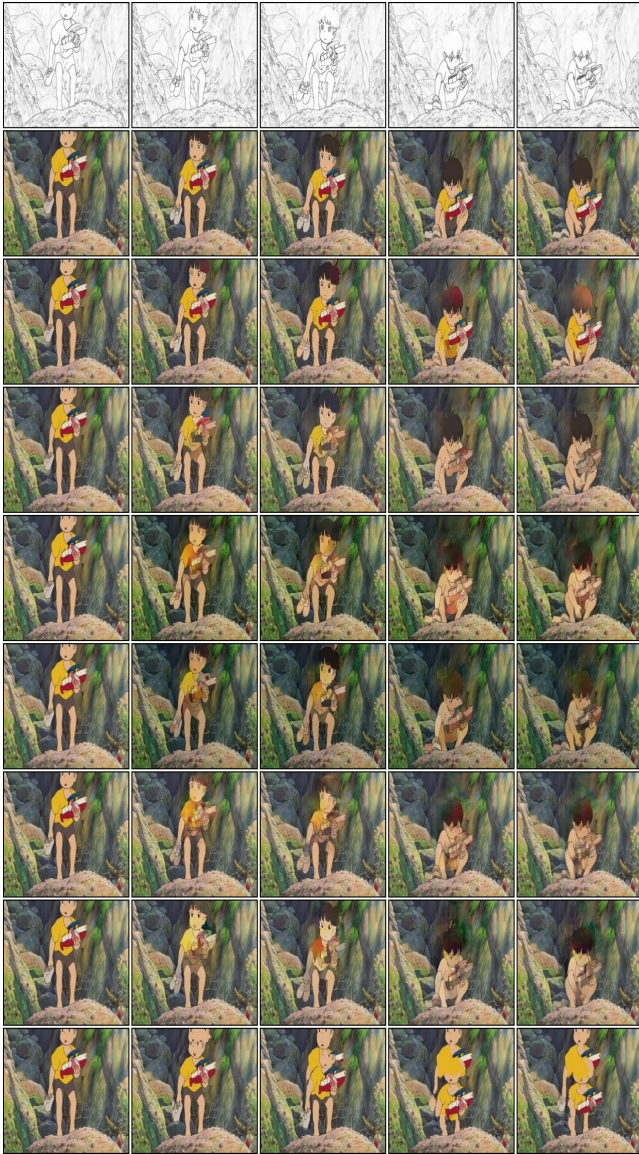


Figure 6: Example of all the compared method at stride=5, from top to bottom is the ground truth and the results of LCMN, LCMN (w/o CM), TCVC (our loss), TCVC, Pix2Pix (with ref/our loss), Pix2Pix (with ref), DeepAnalogy. The first column of each rows is the origin colored image, and the successive colour is the predicted frame conditioned on the first colored reference. The example sequence is from the film *Ponyo*

### 4.3 Comparison against the State-of-the-Art

We compare our method with TCVC [27], Pix2Pix [11] and DeepAnalogy [15]. In order to adjust the Pix2Pix model to fit exemplar-based sketch colorization task, we directly concatenate the reference to the input just as the same as the strategy introduced in TCVC. As we can see in Table 1, 2, 3, the TCVC and Pix2Pix model is no better

Table 2: PSNR/SSIM result of frame sequence with stride=5

method	frame1( $iv:5$ )	frame2( $iv:10$ )	frame3( $iv:15$ )	frame4( $iv:20$ )
LCMN	<b>27.88/0.9669</b>	<b>26.84/0.9595</b>	<b>26.03/0.9539</b>	<b>25.59/0.9506</b>
LCMN(w/o CM)	26.21/0.9559	25.02/0.9459	24.23/0.9388	23.73/0.9336
TCVC(our loss)	21.98/0.8954	21.44/0.8872	21.04/0.8810	20.78/0.8769
TCVC	22.22/0.8979	21.71/0.8905	21.30/0.8843	21.02/0.8801
Pix2Pix(with ref/our loss)	25.44/0.9389	24.11/0.9274	23.25/0.9119	22.77/0.9141
Pix2Pix(with ref)	24.41/0.9331	23.15/0.9196	22.35/0.9098	21.90/0.9037
DeepAnalogy	24.77/0.9567	23.59/0.9462	22.67/0.9401	22.28/0.9364

Table 3: PSNR/SSIM result of frame sequence with stride=10

method	frame1( $iv:10$ )	frame2( $iv:20$ )	frame3( $iv:30$ )	frame4( $iv:40$ )
LCMN	<b>26.30/0.9586</b>	<b>25.16/0.9494</b>	<b>24.58/0.9440</b>	<b>24.18/0.9397</b>
LCMN(w/o CM)	23.97/0.9395	22.80/0.9261	22.24/0.9190	21.88/0.9134
TCVC(our loss)	21.44/0.8872	20.77/0.8769	20.46/0.8713	20.20/0.8664
TCVC	21.70/0.8937	21.01/0.8834	20.69/0.8782	20.43/0.8735
Pix2Pix(with ref/our loss)	24.11/0.9274	22.77/0.9141	22.13/0.9066	21.69/0.9005
Pix2Pix(with ref)	23.15/0.9196	21.90/0.9037	21.34/0.8957	20.95/0.8890
DeepAnalogy	23.59/0.9462	22.28/0.9364	21.47/0.9241	21.07/0.9199

Table 4: Time spent for colorize one frame

method	LCMN	LCMN(w/o CM)	TCVC	Pix2Pix	DeepAnalogy
time(s)	0.90	0.82	0.22	0.17	7.24

than LCMN both with our loss or the original loss, especially when the frame interval is big, since they are constrained by the locality of their generator. Since small changes between coherent sketch frames can be colorized by the local ability of U-Net, the Pix2Pix model can reach a good performance when interval=1. With the increasing of the stride between frames, however, the performance decreases dramatically. When we replace the loss of Pix2Pix to our loss, the consistency of the colorization has improved. This is because the GAN loss is learned from the whole data set, which will introduce some color bias when considering a single generated image. The results of the TCVC are unstable as some results suffer from a color inconsistency. As can be seen in row 5 and 6 of Figure 5, TCVC model tends to change the color slightly even at unchanged sketch positions.

The original DeepAnalogy suppose to utilize  $x_A$  and  $y_B$  to predict  $x_B$ . DeepAnalogy calculates the patch matching in the same image domain to guarantee the matching precision, namely, matching between DCNN features of  $x_A$  and  $y_A$  and DCNN features of  $x_B$  and  $y_B$  respectively. In the original version, the feature of  $x_B$  ( $y_A$ ) is estimated by fusing the feature of  $x_A$  ( $y_B$ ) and the previous layers' matching result. But every reference colored image has its corresponding sketch image in our task, so we eliminate the procedure of estimating the feature of  $y_A$  and replace it with the real feature of  $y_A$  layer-wise. Simultaneously, the procedure of estimating the feature of  $x_B$  is still kept unchanged. The result of DeepAnalogy can reach a good performance when the change between frames is small (interval=1), but more matching errors show up with the increasing of motion intensity. Different from learnable and task-specified deep features extracted by LCMN, the VGG features of the sparse sketch can not provide an adequate semantic representation for the correct patch match. Because of the lack of considering semantic





Figure 7: Example of all the compared method at stride=10, from top to bottom is the ground truth and the results of LCMN, LCMN (w/o CM), TCVC (our loss), TCVC (with ref/our loss), Pix2Pix (with ref), DeepAnalysis. The first column of each rows is the origin colored image, and the successive colour is the predicted frame conditioned on the first colored reference. The example sequence is from the film *Porco Rosso*

correctness which can be learned by generator based method from abundant images in the training dataset, the result of DeepAnalysis suffers from a serious discontinuity and distortion (as can be seen in row 9 in Figure 5, row 9 in Figure 7). As shown in Table 4, the calculating speed of DeepAnalysis is far slower than other methods, since the patch match and the reconstruction of the feature of  $x_B$  in each layers are both time-consuming.

## 5 CONCLUSION

In this paper, we first introduced a sketch correlation matching model that can mine abundant and comparable feature representations. Then we integrated the CM model into a U-Net generator by designing two extra line art and colored frame encoders. Furthermore, we collected a sequential colorization dataset and designed a strategy to get the training frame pair with intense and diverse variations to learn a more robust line art correlation. Experiments showed that our LCMN can effectively improve the in-between consistency and quality, especially when big and complicated motion occurs.

## REFERENCES

- [1] Patricia S. Abril and Robert Plant. 2019. Anime Industry Report 2018 Summary. (Jan. 2019). <https://aja.gr.jp/english/japan-anime-data>
- [2] Lorenzo Baraldi, Costantino Grana, and Rita Cucchiara. 2015. Shot and scene detection via hierarchical clustering for re-using broadcast video. In *International Conference on Computer Analysis of Images and Patterns*. Springer, 801–811.
- [3] Wengling Chen and James Hays. 2018. Sketchygan: Towards diverse and realistic sketch to image synthesis. In *Proceedings of the IEEE Conference on Computer Vision and Pattern Recognition*. 9416–9425.
- [4] Li Cheng, SV N Vishwanathan, and Xinhua Zhang. 2008. Consistent image analogies using semi-supervised learning. In *2008 IEEE Conference on Computer Vision and Pattern Recognition*. IEEE, 1–8.
- [5] Yuanzheng Ci, Xinzhu Ma, Zhihui Wang, Haojie Li, and Zhongxuan Luo. 2018. User-guided deep anime line art colorization with conditional adversarial networks. In *Proceedings of the 26th ACM international conference on Multimedia*. 1536–1544.
- [6] Kevin Frans. 2017. Outline colorization through tandem adversarial networks. *arXiv preprint arXiv:1704.08834* (2017).
- [7] Chie Furusawa, Kazuyuki Hiroshiba, Keisuke Ogaki, and Yuri Odagiri. 2017. Comicolorization: semi-automatic manga colorization. In *SIGGRAPH Asia 2017 Technical Briefs*. 1–4.
- [8] Kaiming He, Xiangyu Zhang, Shaoqing Ren, and Jian Sun. 2016. Deep residual learning for image recognition. In *Proceedings of the IEEE conference on computer vision and pattern recognition*. 770–778.
- [9] Paulina Hensman and Kiyoharu Aizawa. 2017. cGAN-based manga colorization using a single training image. In *2017 14th IAPR International Conference on Document Analysis and Recognition (ICDAR)*, Vol. 3. IEEE, 72–77.
- [10] Aaron Hertzmann, Charles E Jacobs, Nuria Oliver, Brian Curless, and David H Salesin. 2001. Image analogies. In *Proceedings of the 28th annual conference on Computer graphics and interactive techniques*. 327–340.
- [11] Phillip Isola, Jun-Yan Zhu, Tinghui Zhou, and Alexei A Efros. 2017. Image-to-image translation with conditional adversarial networks. In *Proceedings of the IEEE conference on computer vision and pattern recognition*. 1125–1134.
- [12] Justin Johnson, Alexandre Alahi, and Li Fei-Fei. 2016. Perceptual losses for real-time style transfer and super-resolution. In *European conference on computer vision*. Springer, 694–711.
- [13] Hyunsu Kim, Ho Young Jhoo, Eunhyeok Park, and Sungjoo Yoo. 2019. Tag2pix: Line art colorization using text tag with secant and changing loss. In *Proceedings of the IEEE International Conference on Computer Vision*. 9056–9065.
- [14] Chuan Li and Michael Wand. 2016. Combining markov random fields and convolutional neural networks for image synthesis. In *Proceedings of the IEEE Conference on Computer Vision and Pattern Recognition*. 2479–2486.
- [15] Jing Liao, Yuan Yao, Lu Yuan, Gang Hua, and Sing Bing Kang. 2017. Visual attribute transfer through deep image analogy. *arXiv preprint arXiv:1705.01088* (2017).
- [16] Yifan Liu, Zengchang Qin, Zhenbo Luo, and Hua Wang. 2017. Auto-painter: Cartoon image generation from sketch by using conditional generative adversarial networks. *arXiv preprint arXiv:1705.01908* (2017).
- [17] Preferred Networks. 2017. paintschainer. (2017). [https://petalica-paint.pixiv.dev/index\\_zh.html](https://petalica-paint.pixiv.dev/index_zh.html)
- [18] Gioacchino Noris, Daniel Šykora, Stelian Coros, Brian Whited, Maryann Simons, Alexander Hornung, Marcus Gross, and Robert W Sumner. 2011. Temporal noise control for sketchy animation. In *Proceedings of the ACM SIGGRAPH/Eurographics Symposium on Non-Photorealistic Animation and Rendering*. 93–98.
- [19] Alec Radford, Luke Metz, and Soumith Chintala. 2015. Unsupervised representation learning with deep convolutional generative adversarial networks. *arXiv preprint arXiv:1511.06434* (2015).
- [20] Olaf Ronneberger, Philipp Fischer, and Thomas Brox. 2015. U-net: Convolutional networks for biomedical image segmentation. In *International Conference on Medical image computing and computer-assisted intervention*. Springer, 234–241.



- [21] Masaki Saito and Yusuke Matsui. 2015. Illustration2vec: a semantic vector representation of illustrations. In *SIGGRAPH Asia 2015 Technical Briefs*. 1–4.
- [22] Kazuhiro Sato, Yusuke Matsui, Toshihiko Yamasaki, and Kiyoharu Aizawa. 2014. Reference-based manga colorization by graph correspondence using quadratic programming. In *SIGGRAPH Asia 2014 Technical Briefs*. 1–4.
- [23] Wenzhe Shi, Jose Caballero, Ferenc Huszár, Johannes Totz, Andrew P Aitken, Rob Bishop, Daniel Rueckert, and Zehan Wang. 2016. Real-time single image and video super-resolution using an efficient sub-pixel convolutional neural network. In *Proceedings of the IEEE conference on computer vision and pattern recognition*. 1874–1883.
- [24] Zhijun Song, Jun Yu, Changle Zhou, and Meng Wang. 2013. Automatic cartoon matching in computer-assisted animation production. *Neurocomputing* 120 (2013), 397–403.
- [25] Daniel Šykora, Mirela Ben-Chen, Martin Čadik, Brian Whited, and Maryann Simmons. 2011. TexToons: practical texture mapping for hand-drawn cartoon animations. In *Proceedings of the ACM SIGGRAPH/Eurographics Symposium on Non-Photorealistic Animation and Rendering*. 75–84.
- [26] Daniel Šykora, John Dingliana, and Steven Collins. 2009. As-rigid-as-possible image registration for hand-drawn cartoon animations. In *Proceedings of the 7th International Symposium on Non-Photorealistic Animation and Rendering*. 25–33.
- [27] Harrish Thasarathan, Kamyar Nazeri, and Mehran Ebrahimi. 2019. Automatic temporally coherent video colorization. In *2019 16th Conference on Computer and Robot Vision (CRV)*. IEEE, 189–194.
- [28] Zhou Wang, Alan C Bovik, Hamid R Sheikh, and Eero P Simoncelli. 2004. Image quality assessment: from error visibility to structural similarity. *IEEE transactions on image processing* 13, 4 (2004), 600–612.
- [29] Saining Xie, Ross Girshick, Piotr Dollár, Zhuowen Tu, and Kaiming He. 2017. Aggregated residual transformations for deep neural networks. In *Proceedings of the IEEE conference on computer vision and pattern recognition*. 1492–1500.
- [30] Jun Xing, Li-Yi Wei, Takaaki Shiratori, and Koji Yatani. 2015. Autocomplete hand-drawn animations. *ACM Transactions on Graphics (TOG)* 34, 6 (2015), 1–11.
- [31] Fisher Yu and Vladlen Koltun. 2015. Multi-scale context aggregation by dilated convolutions. *arXiv preprint arXiv:1511.07122* (2015).
- [32] Matthew D Zeiler and Rob Fergus. 2014. Visualizing and understanding convolutional networks. In *European conference on computer vision*. Springer, 818–833.
- [33] Lvmin Zhang, Yi Ji, Xin Lin, and Chunping Liu. 2017. Style transfer for anime sketches with enhanced residual u-net and auxiliary classifier gan. In *2017 4th IAPR Asian Conference on Pattern Recognition (ACPR)*. IEEE, 506–511.
- [34] Lvmin Zhang, Chengze Li, Tien-Tsin Wong, Yi Ji, and Chunping Liu. 2018. Two-stage sketch colorization. *ACM Transactions on Graphics (TOG)* 37, 6 (2018), 1–14.
- [35] Haichao Zhu, Xueting Liu, Tien-Tsin Wong, and Pheng-Ann Heng. 2016. Globally optimal toon tracking. *ACM Transactions on Graphics (TOG)* 35, 4 (2016), 1–10.
- [36] Jun-Yan Zhu, Taesung Park, Phillip Isola, and Alexei A Efros. 2017. Unpaired image-to-image translation using cycle-consistent adversarial networks. In *Proceedings of the IEEE international conference on computer vision*. 2223–2232.